

Characterization of Network Structures in UV-Cured Acrylic Ester Resin by Pyrolysis–Gas Chromatography in the Presence of Organic Alkali

Hideki Matsubara,[†] Asuka Yoshida,[‡] Yosuke Kondo,[‡] Shin Tsuge,[‡] and Hajime Ohtani^{*‡}

Aichi Industrial Technology Institute, Kariya 448-0003, Japan, and Department of Applied Chemistry, Graduate School of Engineering, Nagoya University, Nagoya, 464-8603, Japan

Received December 26, 2002; Revised Manuscript Received May 6, 2003

ABSTRACT: Network structures in the UV-cured resin prepared from bifunctional poly(ethylene glycol) diacrylate (PEDA) were characterized by pyrolysis gas–chromatography (Py-GC) in the presence of organic alkali, tetramethylammonium hydroxide (TMAH). The pyrogram of the uncured prepolymer compound consisting of PEDA and a photoinitiator, 2-methyl-1-[4-(methylthio)phenyl]-2-morpholinopropanone-1 (MMMP), were comprised of specific products such as methyl acrylate (MA), intact MMMP, and a series of dimethyl ethers of poly(ethylene glycol) oligomers. Meanwhile, on the pyrogram of the cured resin prepared with the prepolymer compound through UV irradiation, minor but distinctive peaks of methyl acrylate oligomers (MA oligomers) were additionally observed, while those of MA and MMMP considerably lowered as a result of cross-linking formation. The MA oligomers were formed through reactive pyrolysis and methylation selectively occurred at ester linkages of PEDA moieties in the UV-cured resin and were attributed to the sequences of network junctions in cross-linking structure. The observed peak intensities of the MA oligomers thus observed were interpreted in terms of the chain length distribution of network junctions in the cured resin.

Introduction

Ultraviolet (UV)-induced photopolymerization is currently utilized in the various industrial field such as paints, inks, adhesives, coatings for optical fibers and disks, photoresist, and three-dimensional stereolithography.^{1–3} To improve the performance of the UV-curable resins, it is requested to elucidate both the kinetics of photopolymerization and the chemical structures of the cured polymers. The photopolymerization kinetics of UV-curable resins have been extensively studied over the years.^{4–6} For example, the influence of reaction conditions such as polymerization temperature, light intensity, composition, and structure of acrylic esters on the curing behavior has been investigated in detail using various techniques such as real-time infrared spectroscopy^{4–7} and isothermal differential scanning calorimetry (photocalorimetry).^{4–6,8}

However, photopolymerization processes including autoacceleration, autodeceleration, and limited mobility of active species often cause complex microstructures such as cross-linking, pendant double-bond, cycles, unreacted prepolymer, and microgels.^{1,3,4,9} Therefore, it is not an easy task to characterize the resultant network structures of photocured resins in detail. Although the high-resolution solution NMR is a powerful tool for the characterization of microstructures in various polymers,^{10,11} it cannot be applied to the detailed analysis of the cross-linked UV-cured resins because of their insoluble nature. On the other hand, solid-state NMR has been utilized to study the structure heterogeneity in the polymerization of multifunctional acrylates and

methacrylates.^{12–14} Recently, the network structure of UV-cured acrylate was also analyzed by solid-state NMR in terms of the conversion, mean cross-link density, the contribution of side reactions, and the spatial distribution of cross-links.^{5,15–17} However, this technique is generally time-consuming and requires relatively large amounts of sample. Moreover, the characterization of the microstructures such as kinetic chain length of network junctions has not been achieved by the solid-state NMR yet for the rigidly cross-linked UV-cured resins because of insufficient resolution.

Meanwhile, pyrolysis–gas chromatography (Py-GC) has been utilized as a powerful tool for the characterization of intractable polymeric materials such as vulcanized rubbers¹⁸ and polystyrene gels.¹⁹ Moreover, recently developed Py-GC in the presence of organic alkali such as tetramethylammonium hydroxide (TMAH) enables to characterize insoluble cross-linking polymers containing polar components such as epoxy resins.^{20,21} More recently, detailed characterization of branched and cross-linking structures in the polycarbonate^{22,23} and the liquid crystalline aromatic polyester²⁴ samples insolubilized through their thermal treatment has been achieved by using this technique. Furthermore, Py-GC using TMAH has also been successfully applied to the compositional analysis of multicomponent UV-cured resins.²⁵ In this work, the reactive Py-GC in the presence of TMAH was extendedly applied to study the network structures in the UV-cured acrylic ester resin prepared from poly(ethylene glycol) diacrylate in the presence of an α -aminoalkylphenone-type photoinitiator mainly by focusing on the chain length distribution of network junctions.

Experimental Section

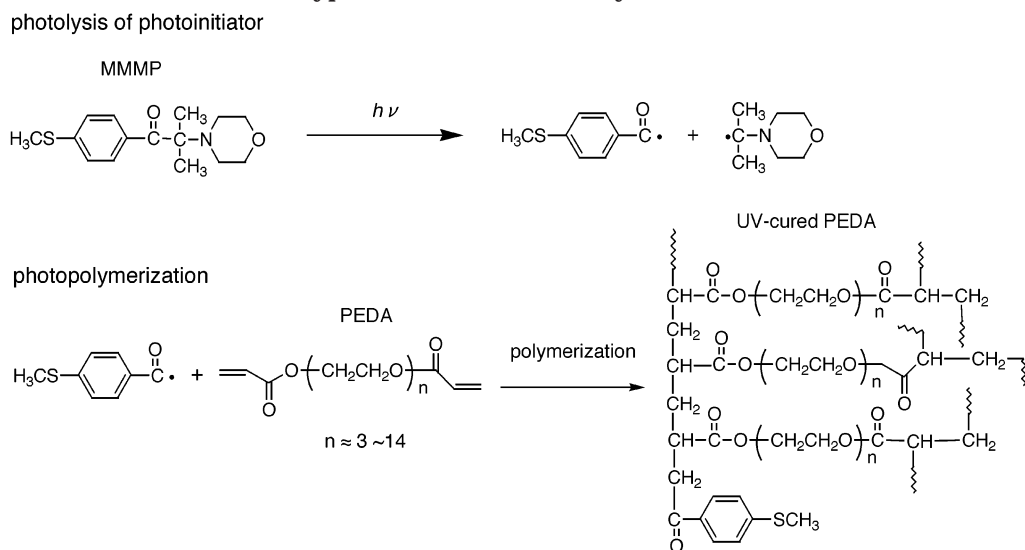
Samples. Poly(ethylene glycol) diacrylate (PEDA) with weight-average molecular weight of about 500 was obtained

[†] Aichi Industrial Technology Institute.

[‡] Nagoya University.

* To whom correspondence should be addressed: e-mail hajime@apchem.nagoya-u.ac.jp; Tel +81-52-789-3560; Fax +81-52-789-4666.

Scheme 1. Typical Formation Pathway of UV-Cured PEDA



from Nippon Kayaku Co. Ltd. The photoinitiator, 2-methyl-1-[4-(methylthio)phenyl]-2-morpholinopropanone-1 (MMMP), obtained from CIBA Specialty Chemicals Co. Ltd. was used without further purification. Scheme 1 shows a typical mechanism of UV-induced photopolymerization using a combination of PEDA and MMMP. By absorbing UV light, MMMP undergoes intramolecular splitting into radicals. The major active species are considered to be benzoyl radicals,^{4,26} which initiate free radical polymerization of terminal acryloyl groups in the prepolymers, while the contributions of the counter radicals to the initiation reactions are considered to be negligibly small. Although some contribution of cyclization reactions in curing between the propagating radicals and pendant double bonds was suggested by Jennie et al.,⁹ they were not considered in this scheme.

The procedure for preparing UV-cured resin samples is basically the same as described in our previous paper.²⁵ Prepolymer was compounded by dissolving MMMP into PEDA at 70 °C (PEDA:MMMP = 100:3). Then, the prepolymer compound was applied to glass plate to give a 10 μ m thick film using a bar applicator.²⁷ UV-curing was carried out in air by passing the prepolymer film on the glass plate through a conveyor system, by which the film is exposed to a 80 W/cm medium-pressure mercury lamp (80 W/cm and total output 2 kW) having an infrared cutoff filter. The dosage for a single pass was determined to be 75 mJ/cm² by a UV integrator (EYE Graphics UVPF-36, wavelength range = 300–390 nm). The irradiation was repeated three times until the sample film hardened sufficiently to give a tack-free surface. The total dosage for preparing the UV-cured PEDA was 225 mJ/cm².

Reactive Py-GC Measuring Conditions. The equipment and procedure for reactive Py-GC are almost the same as used in our previous paper.²⁵ A vertical microfurnace type pyrolyzer (Frontier Lab model PY-2010D) was directly attached to the inlet of a gas chromatograph (Hewlett-Packard HP5890) equipped with a metal capillary column [Frontier Lab Ultra ALLOY⁺, 5, 30 m \times 0.25 mm i.d., coated with a 0.25 μ m film of cross-linked poly(5% diphenyl)dimethylsiloxane] and a flame ionization detector (FID).

An aqueous solution (25 wt %) of tetramethylammonium hydroxide [(CH₃)₄NOH; TMAH] (Aldrich) was used as the reagent for reactive Py-GC. About 100 μ g of the UV-cured sample or the prepolymer compound was placed in the platinum sample cup together with 4 μ L of the aqueous solution of TMAH. As for the cured resin, the sample film was cryomilled into a fine powder by a freezer mill (Spex 6750) at liquid nitrogen temperature prior to Py-GC measurements in order to homogenize the sample and to improve the efficiency of the reaction with the reagent. The sample cup containing the resin sample and the reagent was positioned in the top of the pyrolyzer near room temperature and then dropped into

the continuously heated center at 400 °C.²⁸ The amount of TMAH added corresponds to ca. 20 times that required hydrolyzable ester bonds in the UV-cured PEDA sample under examination. The reactive pyrolysis temperature and the amount of TMAH were empirically optimized so that the highest yield of methyl derivatives of the resin components was obtained instantaneously with minimizing undesirable thermal cleavage except for the ester linkages. The hydrolytical decomposition of the resin sample at 400 °C is known to finish within a short time in the presence of TMAH by accompanying methylation of the products. The reaction products thus formed were rapidly swept from the pyrolyzer to the separation column by a flow of 50 mL/min helium carrier gas. The carrier gas flow was then reduced to 1 mL/min at the inlet of the capillary column by means of a splitter. The column temperature was initially set at 35 °C for 6 min to separate the relatively low-boiling-point degradation products from large amounts of methanol and trimethylamine formed from excess TMAH and then programmed up to 340 °C at a rate of 5 °C/min. Identification of the peaks on the pyrograms was performed by use of a Py-GC/MS system (JEOL Automass System II equipped with the same microfurnace pyrolyzer). Both an electron impact ionization source and a chemical ionization one with isobutane as the reagent gas were used in the analysis.

Results and Discussion

Reactive Pyrolysis Behavior of Prepolymer Compound and Its UV-Cured Resin. Figure 1 shows the pyrograms of the prepolymer compound containing MMMP (a) and its UV-cured resin (b) obtained by reactive pyrolysis in the presence of TMAH at 400 °C. The assignments of the mainly observed peaks are summarized in Table 1 along with their chemical structures and the effective carbon numbers corresponding to the FID response empirically calculated.²⁹ On both pyrograms, a series of poly(ethylene glycol) dimethyl ether (DM_n labeled by solid circles (●): $n = 3-14$, which correspond to the numbers of the ethylene oxide units) reflecting a PEDA skeleton were mainly observed. In addition, methyl acrylate (MA), MMMP, and two series of minor products relating to PEDA skeleton, MM_n designated by solid squares (■) and ME_n by solid triangles (▲), were also more or less formed in both pyrograms.

Among these products, MA and DM₃–DM₁₄ were considered to be formed through hydrolysis of ester linkages in PEDA followed by simultaneous methyl-

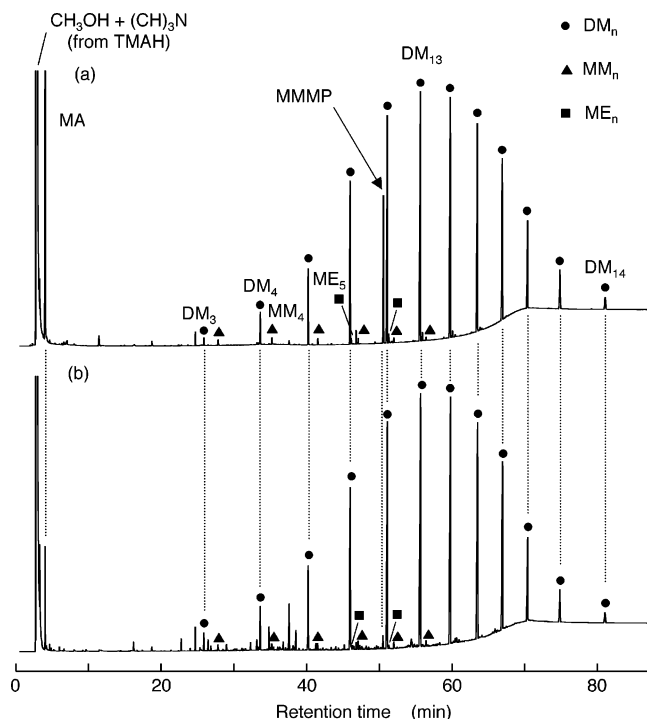


Figure 1. Pyrograms of UV-curable resin samples observed at 400 °C in the presence of TMAH: (a) prepolymer compound containing MMMP; (b) UV-cured resin.

Table 1. Pyrolysis Products Commonly Formed from the Prepolymer Compound and Its Cured Resin

Peak codes ^a	Chemical structure	Effective carbon numbers ^b
MMMP		13.15 ^c
MA		2.65
DM _n (<i>n</i> = 3 ~ 14)	$\text{H}_3\text{CO}-(\text{CH}_2\text{CH}_2\text{O})_n-\text{CH}_3$	$1.2n + 1.2$
MM _n	$\text{H}_3\text{CO}-(\text{CH}_2\text{CH}_2\text{O})_n-\text{H}$	$1.2n + 0.2$
ME _n	$\text{H}_3\text{CO}-(\text{CH}_2\text{CH}_2\text{O})_n-\text{C}_2\text{H}_5$	$1.2n + 2.2$

^a Peak codes correspond to those on pyrograms in Figures 1 and 2. ^b Effective carbon number for molar sensitivity correction of FID response.²⁹ ^c The effective carbon number of MMMP was calculated without considering effect of sulfur atom.

ation. Meanwhile, MM_n may be formed due to partial methylation after hydrolysis of the ester linkages, whereas ME_n might be produced with the contributions of pyrolytic cleavage at the CH₂-O bond in PEDA chain, although the total amounts of MM_n and ME_n on the pyrograms were negligibly small compared to those of DM_n. On the other hand, MMMP might be originated from the intact photoinitiator present in the samples, which hardly reacted with TMAH but vaporized without any thermal degradation during reactive pyrolysis process under the given conditions.

On the both pyrograms, DM_n's reflecting a PEDA skeleton were observed as main products with similar distributions. MA and MMMP from the UV-cured resin

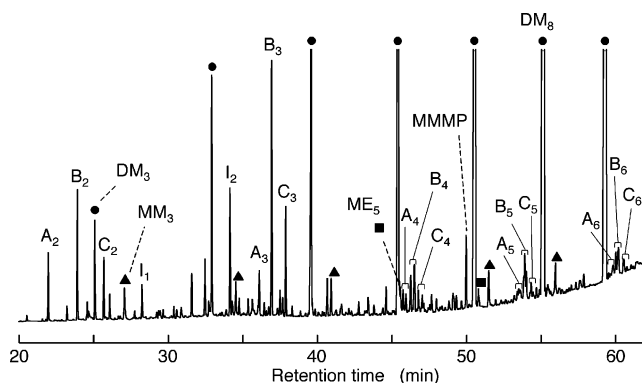


Figure 2. Expanded pyrogram of the UV-cured resin.

Table 2. Pyrolysis Products Formed only from the UV-Cured Resin

Peak codes ^a	Chemical structure	Effective carbon numbers ^b
I ₁		8.2 ^c
I ₂		7.75 ^c
A _m (<i>m</i> = 2 ~ 6)		$2.75m - 1$
B _m (<i>m</i> = 2 ~ 6)		$2.75m - 0.1$
C _m (<i>m</i> = 2 ~ 6)		$2.75m + 0.8$

^a Peak codes correspond to those on the pyrogram in Figure 2. ^b Effective carbon number for molar sensitivity correction of FID response.²⁹ ^c The effective carbon numbers of I₁ and I₂ were calculated without considering the effect of the sulfur atom.

(Figure 1b) were yielded in markedly smaller amounts than those from the prepolymer compound. Furthermore, the pyrogram of the UV-cured resin contained various minor but distinctive peaks which were absent on that of the prepolymer compound. Therefore, they can be mostly assigned to the pyrolysis products arising from the network structure of the UV-cured resin sample.

Figure 2 shows the expanded pyrogram of the UV-cured resin with focusing on the minor products characteristic of the network structure observed in Figure 1b. The peak assignments for the minor products exclusively formed from the UV-cured resin are summarized in Table 2 along with their chemical structures and effective carbon numbers. Among these products, the fragments related to MMMP moieties incorporated into the polymer chain (I₁ and I₂) were clearly observed in addition to a series of methyl acrylate (MA) oligomers (A_m, B_m, and C_m; *m* = 2–6) which might be the characteristic pyrolysates reflecting the network struc-

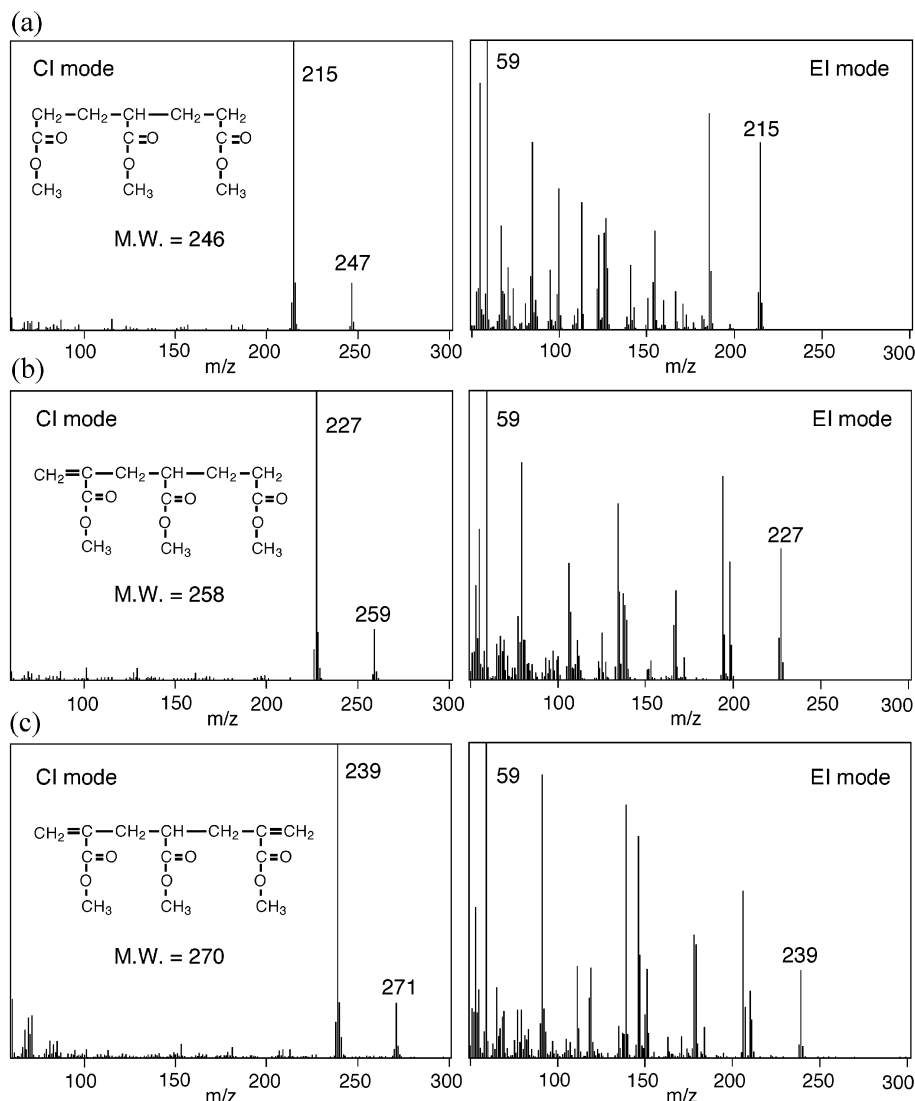


Figure 3. CI and EI mass spectra of (a) peak A₃, (b) peak B₃, and (c) peak C₃ on the pyrogram of Figure 2.

ture. These products were identified to be methyl 4-(methylthio)benzoate (I_2) formed through hydrolysis and methyl esterification of the initiator fragment incorporated in the resin structure and its byproduct, methyl 4-(methylthio)benzyl ether (I_1). However, the fact that any pyrolysates including the other counter-constituent of the initiator, that is, the morpholino group, were not observed at all supports the general conception that photopolymerization in the presence of MMMP is initiated predominantly by the benzoyl radical.^{4,19} Furthermore, intact MMMP was still observed as a minor constituent, suggesting that the initiator partially remained in the UV-cured resin. The amount of residual MMMP in the UV-cured resin was estimated to be about 8% of that in the prepolymer compound under the given conditions by comparing the peak intensities of MMMP in the pyrograms before and after UV-curing.

Figure 3 shows CI- and EI-mass spectra of the representative peaks (A₃, B₃, and C₃) among the MA oligomers observed between ca. 36 and 38 min in the pyrogram of the cured resin. In every EI-mass spectrum, base fragment ion at $m/z = 59$ ([CH₃OCO]⁺) indicates these products have methyl ester groups. In the CI-mass spectrum of A₃ (Figure 3a), the quasi-molecular ion [M + H]⁺ was observed at $m/z = 247$ together with a base

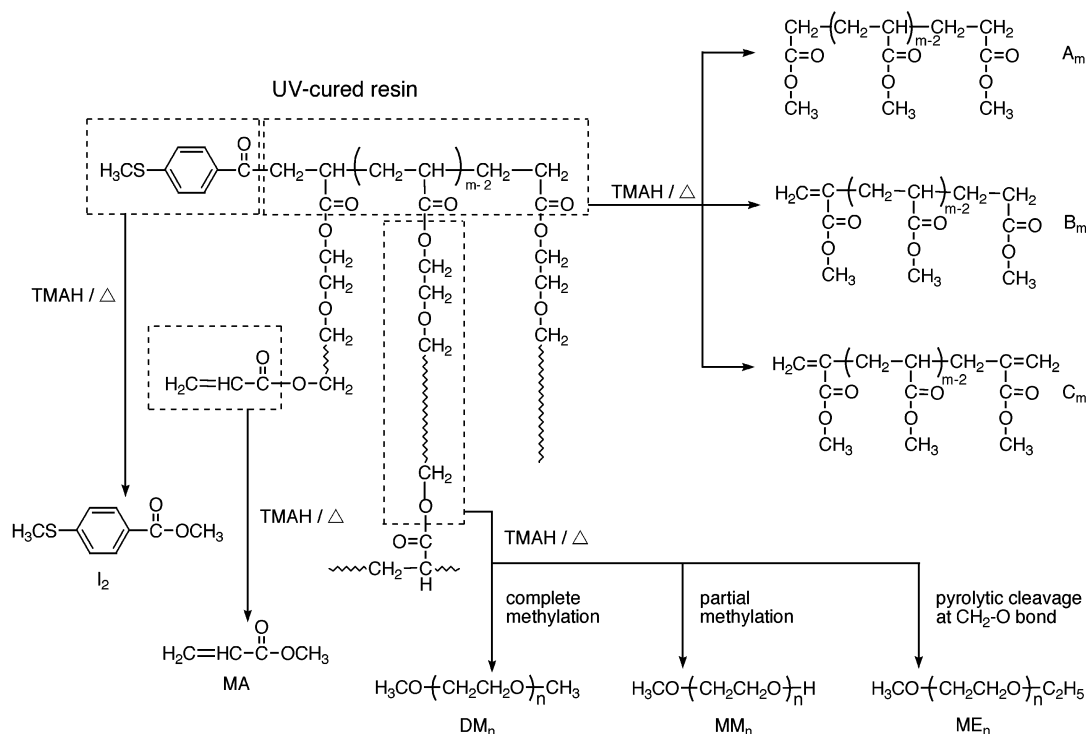
peak corresponding to $[M - OCH_3]^+$ ($m/z = 215$). Consequently, A_3 can be assigned to be a trimer of methyl acrylate (MA trimer) without vinylidene terminal. Similarly, B_3 and C_3 were assigned to MA trimers with one and two vinylidene terminals, respectively. In a similar manner, MA dimers (A_2 , B_2 , and C_2) to hexamers (A_6 , B_6 , and C_6) were identified as the corresponding homologues with the following molecular weight (MW):

$$\text{MW}(\mathbf{A}_m) = 86m - 12; \quad \text{MW}(\mathbf{B}_m) = 86m;$$

$$\text{MW}(C_m) = 86m + 12$$

where m is the number of polymerization degree (2–6), and 86 corresponds to molecular weight of a methyl acrylate unit in the oligomer chain. Here, it should be noted that plural peaks having the same molecular weight were observed in tetramer and the larger oligomer regions. This observation might be attributed to the formation of diastereoisomers in the larger MA oligomers, although detailed assignment was not able to be achieved by the corresponding mass spectra.

Scheme 2 summarizes the estimated formation pathway of characteristic products derived from the UV-cured resin by reactive pyrolysis. MA is formed from

Scheme 2. Formation Pathway of Typical Products of UV-Cured Resin after Reactive Pyrolysis

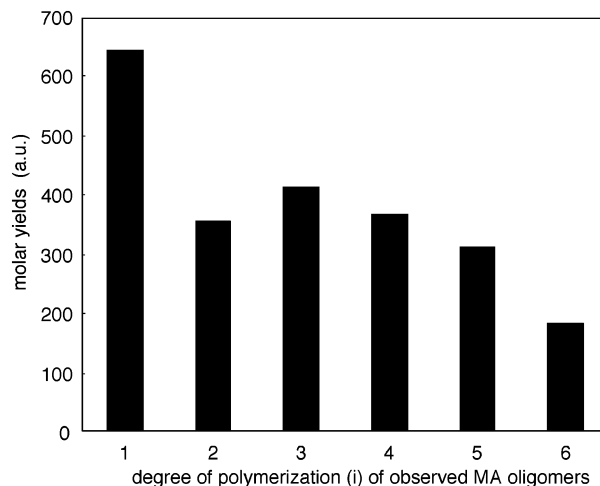
unreacted acryloyl groups of PEDAs moieties, and I₂ is produced from the initiator residue incorporated at the terminal of the polymer chain. Meanwhile, B_m is to be clipped out of a sequence of acryloyl groups constructing the network junctions through the selective hydrolysis and methylation at ester linkages. In fact, B_m series products were chiefly yielded among the three types of the MA oligomers. A_m and C_m are also considered to arise from the polymer chains of the network junctions, although pyrolytic cleavage of C-C bonds might contribute to their formation to some extent. Therefore, the MA oligomers observed in the pyrograms could be correlated to the sequence of the network junctions to form cross-linked and cyclic structures in the UV-cured resin.

Quantitative Evaluation of Network Structure in UV-Cured Resin. The MA oligomers are considered to arise from the polymer chains of network junctions in the UV-cured resin. Therefore, the observed distributions of the MA oligomers could be related to those of the chain length of the junctions, which corresponds to the number of acryloyl groups polymerized by a given radical that initiates a polymer chain.

To estimate the chain length distribution of the repeated acryloyl groups to form a sequence of network junctions, molar yields of the MA units in the given MA oligomers with the degree of polymerization = *m* were calculated as follows:

$$Y_m = m \left(\frac{I_{A_m}}{E_{A_m}} + \frac{I_{B_m}}{E_{B_m}} + \frac{I_{C_m}}{E_{C_m}} \right) \quad (1)$$

where Y_m = molar yields of the observed MA *m*-mers; I_{A_m}, I_{B_m}, I_{C_m} = observed peak intensity of A_m, B_m, C_m; E_{A_m}, E_{B_m}, E_{C_m} = effective carbon numbers of A_m, B_m, C_m indicated in Table 2; and *m* = degree of polymerization.

**Figure 4.** Observed molar yields of MA units in MA and MA oligomers in the pyrogram of the UV-cured resin.

For example, Y₃ is calculated as follows:

$$Y_3 = 3 \left(\frac{I_{A_3}}{7.25} + \frac{I_{B_3}}{8.15} + \frac{I_{C_3}}{9.05} \right)$$

where I_{A₃}, I_{B₃}, and I_{C₃} are peak intensities of A₃, B₃, and C₃ considered to arise from the chain consisting of three bonded acryloyl units (*m* = 3), respectively.

Figure 4 shows the molar yields thus obtained for MA and the MA oligomers in the pyrogram of the UV-cured resin. This result demonstrates that considerable amounts of acryloyl groups remain in the network as pendant groups on polymer chain and terminal ones on residual prepolymer,⁴ which were estimated to be about 10% of the original acryloyls in the prepolymers from the observed peak intensity of MA for the cured resin. Meanwhile, from the yields of the MA oligomers reflecting the network structures, the distributions for the number of PEDAs units composing a sequence of network

junctions can be estimated. These data suggest that acryloyl terminals in the prepolymers might most abundantly form the chain comprised of three PEDA units under the given UV-curing conditions.

However, the molar ratio of total acryloyl units in the observed MA and MA oligomers to total molar amount of DM_n 's on the pyrogram of the UV-cured resin was estimated to be only 0.37 from the peak intensities using a calibration considering the FID responses (effective carbon numbers) summarized in Tables 1 and 2. On the other hand, the corresponding ratio for the prepolymer compound was nearly 2, which accords with the end-group functionality of the PEDA prepolymer. In addition, the fact that the total yields and the distribution of DM_n on the pyrogram of the UV-cured resin were almost equivalent to those of the prepolymer compound suggests that the hydrolysis at the ester linkage of PEDA moieties are considered to proceed quantitatively in the both samples. Therefore, the lower recovery of acryloyl units for the UV-cured resin indicates that fairly large amounts of the longer chains consisting of more than seven acryloyl groups might exist in the UV-cured resin, of which corresponding higher MA oligomers were not observed on the pyrogram mainly because of their lower volatility.

Recently, Burkoth et al. measured the distributions of kinetic chain length of the network junctions of UV-cured dimethacrylated sebacic anhydride polymers by using matrix-assisted laser desorption/ionization-mass spectrometry (MALDI-MS).³⁰ In this case, the cured anhydride polymer was quantitatively hydrolyzed in phosphate buffered saline into poly(methacrylic acid)s, reflecting the sequences of network junctions, which were observed in the MALDI mass spectra in the range between pentamer and 24-mer.

Provided that the UV-cured acrylic ester resins examined in this work are also quantitatively decomposed at the ester linkages, MALDI-MS measurements of the decomposition products should give us useful information even for the longer sequences of the network junctions which are difficult to be observed by reactive Py-GC. In addition, supercritical fluid chromatographic (SFC) measurements of the products might also provide a complementary result for the distribution of the network junctions. In these cases, it is critical to create an appropriate procedure for effective decomposition of the cured acrylic ester resins not only reflecting the kinetic chain length of the network junctions but also amenable to the MALDI-MS and/or SFC measurements. Further studies along these lines are currently in progress.

Acknowledgment. This work was supported in part by the 21st Century COE Program "Nature-Guided

Materials Processing" of the Ministry of Education, Culture, Sports, Science and Technology.

References and Notes

- (1) Kloosterboer, J. G. *Adv. Polym. Sci.* **1988**, *84*, 1–61.
- (2) Garnett, J. L. *Radiat. Phys. Chem.* **1995**, *46*, 925–930.
- (3) Decker, C. *Prog. Polym. Sci.* **1996**, *21*, 593–650.
- (4) Andrzejewska, E. *Prog. Polym. Sci.* **2001**, *26*, 605–665.
- (5) Neckers, D. C.; Jager, W. In *Photoinitiation for Polymerization: UV & EB at the Millenium*; John Wiley and Sons: Chichester, U.K., 1998; Vol. 7, Chapter 3, pp 233–373.
- (6) Fouassier, J. P. In *Photoinitiation, Photopolymerization and Photocuring: Fundamental and Applications*; Hanser/Gardner Publications: Cincinnati, OH, 1995; Chapter 5, pp 145–245.
- (7) Anseth, K. S.; Decker, C.; Bowman, C. N. *Macromolecules* **1995**, *28*, 4040–4043.
- (8) Tryson, G. R.; Shultz, A. R. *J. Polym. Sci., Polym. Phys. Ed.* **1979**, *17*, 2059–2075.
- (9) Jeannine, E. E.; Christopher, N. B. *Macromolecules* **1999**, *32*, 8621–8628.
- (10) Fawcett, A. H.; Hamilton, J. G.; Rooney, J. J. In *Polymer Spectroscopy*; Fawcett, A. H., Ed.; Wiley: Chichester, U.K., 1996; Chapter 1, p 7.
- (11) Ando, I.; Yamano, T.; Asakura, T. *Prog. NMR Spectrosc.* **1990**, *22*, 349–400.
- (12) Allen, P. E. M.; Bennett, D. J.; Hagias, H.; Ross, G. S.; Simon, G. P.; Williams, D. R. G.; Williams, E. H. *Eur. Polym. J.* **1989**, *25*, 785–789.
- (13) Allen, P. E. M.; Simon, G. P.; Williams, D. R. G.; Williams, E. H. *Macromolecules* **1989**, *22*, 809–816.
- (14) Simon, G. P.; Allen, P. E. M.; Bennett, D. J.; Williams, D. R. G.; Williams, E. H. *Macromolecules* **1989**, *22*, 3555–3561.
- (15) Jager, W. F.; Lungu, A.; Chen, D. Y.; Neckers, D. C. *Macromolecules* **1997**, *30*, 780–791.
- (16) Lungu, A.; Neckers, D. C. *Macromolecules* **1995**, *28*, 8147–8152.
- (17) Litvinov, V. M.; Dias, A. A. *Macromolecules* **2001**, *34*, 4051–4060.
- (18) Nakagawa, H.; Tsuge, S.; Murakami, K. *J. Anal. Appl. Pyrolysis* **1986**, *10*, 31–40.
- (19) Nakagawa, H.; Tsuge, S. *Macromolecules* **1985**, *18*, 2068–2072.
- (20) Challinor, J. M. *J. Anal. Appl. Pyrolysis* **1989**, *16*, 323–333.
- (21) Challinor, J. M. *J. Anal. Appl. Pyrolysis* **1991**, *18*, 233–244.
- (22) Oba, K.; Ishida, Y.; Ito, Y.; Ohtani, H.; Tsuge, S. *Macromolecules* **2000**, *33*, 8137–8183.
- (23) Oba, K.; Ohtani, H.; Tsuge, S. *Polym. Degrad. Stab.* **2001**, *74*, 171–176.
- (24) Oba, K.; Ishida, Y.; Ohtani, H.; Tsuge, S. *Polym. Degrad. Stab.* **2002**, *76*, 85–94.
- (25) Matsubara, H.; Yoshida, A.; Ohtani, H.; Tsuge, S. *J. Anal. Appl. Pyrolysis* **2002**, *64*, 159–175.
- (26) Gruber, G. H. *Prog. Polym. Sci.* **1992**, *17*, 953–1004.
- (27) ASTM designation D 4147-82, 1982, American Society for Testing and Materials, Philadelphia, PA.
- (28) Tsuge, S.; Ohtani, H.; Matsubara, H.; Ohsawa, M. *J. Anal. Appl. Pyrolysis* **1987**, *11*, 181–194.
- (29) Jorgenson, A. D.; Picel, K. C.; Stamoudis, V. C. *Anal. Chem.* **1990**, *62*, 683–689.
- (30) Burkoth, K. A.; Anseth, K. S. *Macromolecules* **1999**, *32*, 1438–1444.

MA0217837